RSC Advances

PAPER

View Article Online
View Journal | View Issue

Cite this: *RSC Adv.*, 2016, **6**, 21719

Increasing fluorine concentration to control the microstructure from fullerene-like to amorphous in carbon films

Lifang Zhang,[ab] Jia Wang,[ab] Junyan Zhang[a] and Bin Zhang*[a]

Received 9th January 2016
Accepted 11th February 2016

DOI: 10.1039/c6ra00675b

www.rsc.org/advances

Fluorinated and hydrogenated amorphous carbon (a-C:H:F) films with increasing fluorine content are deposited using a pulsed direct current plasma enhanced chemical vapor deposition technique. The fluorine atomic concentrations of films deposited under CF_4/CH_4 gas with flow ratios of 2 : 1, 4 : 1, 5 : 1, 6 : 1 and 10 : 1 are 4.8%, 5.9%, 6.8%, 12.1% and 15.5%, respectively. As the F content increases, XPS analysis indicates that the C–C bonding structure transforms to form C–CF, C–F and $-CF_2$ groups. TEM images show that the microstructures of the films with lower fluorine contents are constituted by many discontinuous graphite-like and fullerene-like fragments. However, features like interlocking pores and amorphousness strongly prevail in the structures when the proportion of fluorine incorporated into the films increases. The slight increase in I_D/I_G and the up-shift of the G peak obtained from the Raman spectrum indicate the relative increase of the sp^2 configuration and the formation of sp^2-hybridized carbon domains. A deposition mechanism is given to explain the microstructure evolution of the a-C:H:F films upon increasing the fluorine content.

1. Introduction

Fluorinated carbon-based films have attracted much attention because of their prominent properties, such as low surface energy,[1] chemical inertness,[2] controllable hardness,[3] low friction,[4] low dielectric constant[5] and biocompatibility.[6] These properties have been researched and these films have been used in many fields, for example, as an anti-adhesion layer in micro-electro-mechanical system (MEMS) technology, as a thin protecting layer of magnetic media and read/write heads, as an appropriate candidate for thin film transistor liquid crystal displays (TFT-LCD), and as bio- and hemo-compatible films in biomedical devices. Many studies have found that these properties depend on the ratio of F/C content and the ion energies in plasma. It has been demonstrated that the hardness and elastic modulus are reduced consistently upon increasing the fluorine content, while chemical inertness acts in the contrary manner.[7,8] Further mechanism studies indicated that these phenomena are associated with the inner microstructure, while the microstructure is controlled by the film growth, which is determined by ion bombardment.[9] In conclusion, the fluorine content will result in the transformation of the microstructure, and then the microstructure in turn influences the properties. Thus, to determine how these properties change with increasing fluorine content, it is critical to study the structural evolution of fluorinated carbon-based films with increasing fluorine concentration.

Fluorine-doped non-hydrogenated and hydrogenated DLC films can be divided into two categories: a-C:F and a-C:H:F films. Because a-C:H:F films not only have convenience in terms of preparation and selecting a diversity of gas sources, but possess adjustable mechanical, tribological and electronic properties, research has mostly focused on fluorinated and hydrogenated carbon films.[10,11] a-C:H:F films with different fluorine contents have been prepared by two main deposition technologies, namely PECVD and magnetron sputtering. The maximum fluorine contents attainable *via* PECVD and magnetron sputtering are 20 at% and 40 at%, respectively.[12,13] Up to now, speculation over the structural evolution has led to the hypothesis that the film structure changes from diamond-like to a polymer-like structure with the increase in CF_4 partial pressure.[14] Direct images showing the transformation of the structure of a-C:H:F films are still lacking.

In this study, the structural characteristics of films with increasing fluorine concentration are given directly by Transmission Electron Microscopy (TEM). The TEM images indicate that the microstructure changes from well-organized graphite-like and fullerene-like structures to disordered curved fragments upon increasing the fluorine concentration. We clarify the structure transformation mechanisms by combining X-ray photoelectron spectroscopy (XPS) and Raman spectra. Our results point out that the incorporation of fluorine breaks C–C crosslinking bonds and leads to the amorphousness of the

[a]*State Key Laboratory of Solid Lubrication, Lanzhou Institute of Chemical Physics, Chinese Academy of Sciences, Lanzhou 730000, P.R.China*

[b]*University of Chinese Academy of Sciences, Beijing 100049, P. R. China. E-mail: bzhang@licp.cas.cn; Fax: +86-931-4968191; Tel: +86-931-4968191*

microstructure. These results will aid the understanding of how the fluorine content influences film properties.

2. Experimental

2.1 Film deposition

Fluorinated and hydrogenated carbon films were fabricated on Si wafers *via* a pulsed direct current plasma enhanced chemical vapor deposition technique, using CF_4 and CH_4 as gas sources. The parameters of the pulsed direct power device were fixed as follows: (1) applied pulsed bias: −1000 V; (2) pulsed frequency: 20 kHz; (3) duty cycle: 0.6. Prior to deposition, the Si (100) wafers were ultrasonically cleaned in 5 wt% HF and alcohol solution for 20 min in sequence, and then placed on the cathode electrode. Firstly, a base pressure of 7×10^{-4} Pa was attained in the chamber with a turbomolecular pumping system. The Si substrates were then sputter cleaned by argon discharge with 300 sccm gas flow at a working pressure of 5.8 Pa for 30 min. Secondly, an a-C:H buffer layer was deposited to improve the adhesion, the parameters were: $CH_4 = 10$ sccm; Ar = 100 sccm; deposition time = 10 min; film thickness = 300 nm. Thirdly, fluorinated and hydrogenated carbon films with different fluorine concentrations were deposited by varying the gas flow ratio of CF_4/CH_4.

2.2 Characterization of fluorinated and hydrogenated carbon films

The fluorine atomic concentration and carbon chemical states of the deposited films were detected by XPS (Kratos AXIS Ultra DLD), the Al target was used as the X-ray source (the maximum operation power of the Al anode is 600 W). Both plan-view and cross section HRTEM (JEOL 2010) were performed for characterization of the nanostructures of as-deposited films. Raman spectra was obtained using a Jobin Yvon T64000 Raman Spectroscope at the excitation wavelength of the 514 nm Ar laser line and with a spot size of 5 μm, the spectral resolution was less than 1 cm^{-1}.

3. Results and discussion

3.1 Characteristics of fluorine content and chemical states

Fluorinated and hydrogenated carbon films with different fluorine contents in the films were prepared by varying the gas flow ratio of CF_4/CH_4. As shown in Table 1, the fluorine atomic concentration of films deposited at gas flow ratios of 2 : 1, 4 : 1, 5 : 1, 6 : 1, and 10 : 1 are 4.8%, 5.9%, 6.8%, 12.1% and 15.5%, respectively. This indicates that the fluorine atomic concentration in films increases upon increasing the CF_4 gas flow in the gas source. There are always two ways to deposit fluorinated carbon films with different fluorine contents, which are either varying the flow ratio of fluorocarbon gas to carbon sources, or by changing the self-bias voltage.[15] Freire and co-workers[16] showed that the F/C ratio in the film is related to the F/C ratio in the gas mixture. Increasing this value from 1 to 3.2 leads to a progressive increase of the F/C ratio in the film. But when the F/C ratio in the gas mixture is beyond 3.2 or below 1, there appears to be erosion or no fluorine incorporation in the film. In addition, the fluorine content changes from 3 at% to 18 at% upon increasing V_b (fixing the partial pressure of CF_4 at 67%).[17] Thus, controlling the gas ratio of CF_4/CH_4 is a common method to deposit fluorinated and hydrogenated carbon films with different fluorine contents.

Table 1 Intensity ratios of these peaks for films with different fluorine contents

F content (at%)	Intensity (%) Group C–C	C–CF	C–F	CF_2
4.8	82.5	14.41	3.09	—
5.9	80.72	14.1	4	1.18
6.8	77.6	16	4.8	1.6
12.1	73.5	19.8	5.11	1.6
15.5	68.2	23.2	6.6	2

The chemical bonding states of fluorocarbon groups are shown in Fig. 1. The C 1s spectrum can be decomposed into three Gaussian peaks with binding energies of 284.6 eV, 286.6 eV and 289.1 eV, corresponding to C–C, C–CF and C–F bonding states, respectively (Table 1).[18] When the F content increases to 5.9 at%, the $-CF_2$ group at the position of 291.6 eV appears in the film (Fig. 1b).[19] As the fluorine content rises above 6.8 at%, the peak width at half height of the C–F bond becomes sharp, and the intensity of the C–F peak increases (Fig. 1c). Table 1 shows the intensity ratios of these peaks for films with increasing fluorine content. It can be concluded that a gradual transition from a C–C bonding structure to C–CF, C–F and $-CF_2$ groups occurs as the F content increases. When the gas flow ratio of CF_4/CH_4 increases, more C sites bond to single F and form F–C bonds, thus the content of C–C bonds decreases.

It is well known that the C network structure is decided by the deposition process, which correlates with the ion energy and plasma species in the ion impingement.[20] The energy sharing mechanism indicates that the higher the mass ratio of an individual atom to the whole molecule is, the greater the sharing energy of that atom is.[21] Obviously, for CH^{3+} ions this energy is almost totally concentrated in the C atoms, while it is more evenly distributed among all atoms for CF^{3+}. Therefore, for a fixed CF_4 gas flow of 10 sccm, hydrocarbon radicals easily stick onto the surface, resulting in the emergence of deposition. Meanwhile, fluorine coalesces with hydrogen from hydrocarbon radicals to form volatile HF, leaving lots of dangling bonds. These dangling bonds are saturated by –CF and $-CF_2$ ionic groups as the gas flow of CF_4 increases, finally prompting the growth of fluorocarbon groups. The deposition process of a-C:H:F films is described as the substation of hydrogen with fluorine and the growth of a fluorinated carbon structure.[22]

3.2 Microstructure analysis by TEM

There is a general agreement that the increase in fluorine atomic concentration is accompanied by transitions in terms of the type and content of fluorocarbon groups, but how

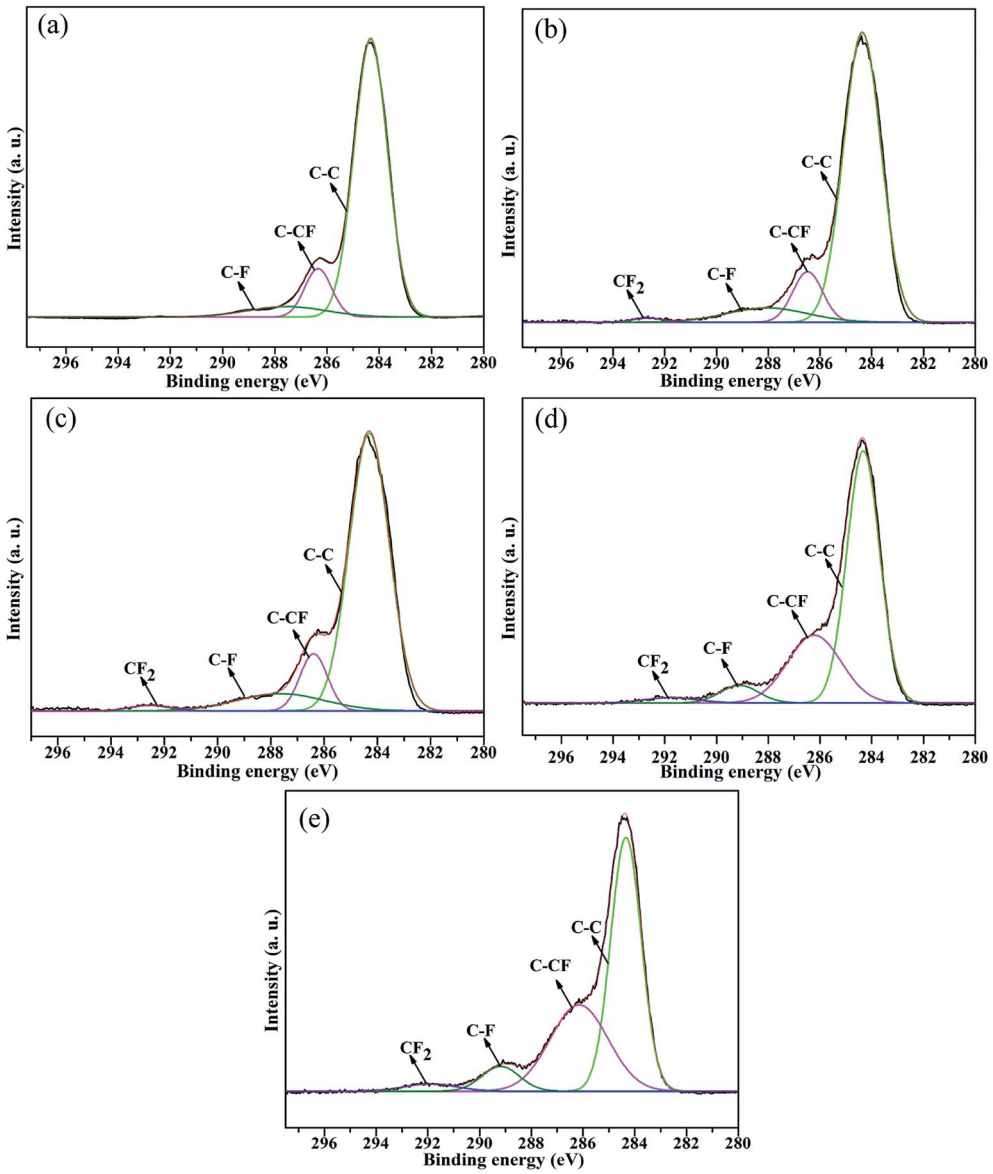

Fig. 1 C 1s spectrum of films deposited at gas flow ratios of (a) 2 : 1, (b) 4 : 1, (c) 5 : 1, (d) 6 : 1, and (e) 10 : 1, whose fluorine contents are 4.8%, 5.9%, 6.8%, 12.1%, and 15.5%, correspondingly.

fluorocarbon groups influence the microstructure still needs to be disclosed. The fluorine concentration has a crucial impact on the bonding states of a-C:H:F fluorine-related groups, and these fluorine-related groups result in the transformation of the microstructure. HRTEM images and SAED patterns are vital to show the microstructural transitions with differing fluorine atomic concentrations. Fig. 2a–c show plan-view HRTEM images of the a-C:H:F films deposited at gas flow ratios of 2 : 1, 6 : 1 and 10 : 1, whose fluorine atomic concentrations correspond to 4.8%, 12.1% and 15.5%, the insets in which are the corresponding selected area electron diffraction (SAED) patterns. The diffuse rings in the SAED patterns demonstrate the non-crystalline or amorphous structure of the films. As seen from Fig. 2a, the fluorinated and hydrogenated carbon film with a low fluorine content of 4.8 at% possesses abundant well-organized graphite-like and fullerene-like domains, displaying discontinuously nanometer size ordered structures embedded in the amorphous carbon matrix. It is also found that one fine ring with a spacing of 2.02 Å appears in the SAED pattern. The value of 2.02 Å matches well with the (101) planar spacing of graphite and confirms the formation of well-organized graphite-like or fullerene-like structures in the as-deposited films. Fig. 2b shows that short and curved fragments interact and interlock to form many holes. The inset SAED patterns of the film show three diffuse rings, the diffuse patterns display three corresponding spacings of 0.95 Å, 3.40 Å, and 5.99 Å. The two rings at 0.95 Å and 5.99 Å coincide with amorphous carbon allotropes of carbon and fluorinated carbon films, while the ring at 3.40 Å matches well with the inter-planar spacing of the hexagonal basal planes in graphite (002), indicative of the presence of

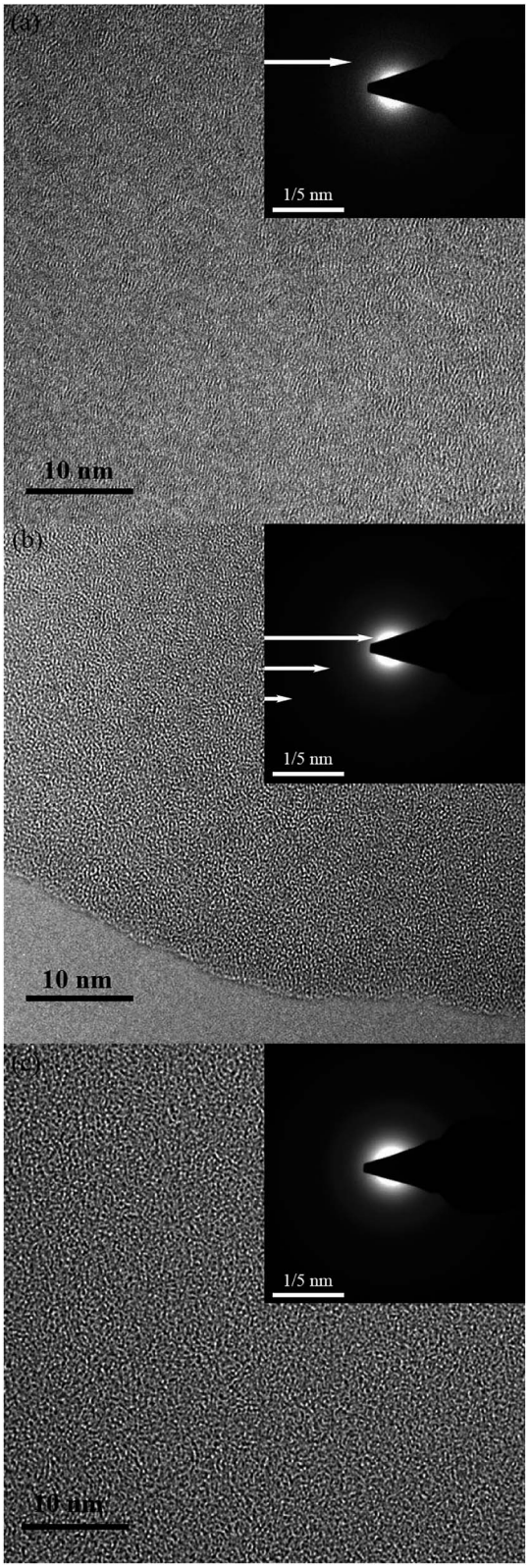

Fig. 2 TEM images of fluorinated and hydrogenated carbon films with different atomic concentrations: (a) 4.8%, (b) 12.1%, (c) 15.5%, the insets in which are the corresponding selected area electron diffraction (SAED) patterns.

defective graphitic planes.[23] With a further increase in fluorine content to 15.5 at%, the fragments become shorter and more curved in Fig. 2c, the a-C:H:F film structure tends to amorphization, and features like interlocking pores and amorphousness strongly prevail.

These phenomena are associated with the change of groups in the deposition process. F terminates C due to its monovalence and high electronegativity, leading to the breaking of C–C crosslink bonding. Meanwhile, fluorine atoms have a larger atomic size compared to H atoms, which modifies the short-range order of the film because of structural effects. Gueorguiev *et al.*[24] studied the role and impact of CF_n ($n = 1, 2$) groups in graphene-like networks. F terminates C and sticks out of the graphene-like network, which disrupts the carbon local microstructure by provoking the formation of characteristic patterns, *i.e.* large rings and chains. The extension of large rings promotes the interlocking of rings at the edge of the network, while the latter leads to the formation of a polymer-like structure. At a low fluorine content, many C sites bond to neighboring C, and the film structure is mainly graphite-like and fullerene-like. Increasing the fluorine content gives rise to C–F bonds and CF_2 bonds. C–F bonds replace C–C bonds and form rings and chains, besides, C with two F atoms terminates crosslink bonding and forms polymer-like chains. Ronning *et al.*[25] deposited amorphous a-C:F films with different microstructures with no crystal regions by changing the ion fraction of $^{19}F^+/^{12}C^+$. They showed that when a low ion fraction of $^{19}F^+/^{12}C^+$ is sputtered, an a-C:F film is formed with diamond-like properties, the formation of $-CF_2$ and $-CF_3$ configurations by increasing the amount of $^{19}F^+$ produces a graphite-like a-C:F film, a further increase in polymer-like CF_2 and CF_3 chains induces the a-C:F film to have a porous structure when the atomic concentration of F exceeds 20% in films. All of these fluorocarbon groups would lead to breakage, bending and interlocking, eventually leading to a transition to amorphization. To conclude, the structure of films with a lower fluorine content is constituted by many discontinuous graphite-like and fullerene-like structures, and greater incorporation of fluorine disrupts these well organized C–C bonding configurations and leads to a higher concentration of defects, tending to amorphization.

3.3 Raman spectra

The Raman measurement is a fast and non-destructive method for the bonding structure characterization of carbon materials. Fig. 3 shows the Raman spectra for the a-C:H:F deposited in this experiment. A broad asymmetric Raman band, which represents the typical features of conventional non-crystalline carbon films, could be observed in the wavenumber range of 800–2000 cm^{-1}.[26] The Raman spectrum can be deconvoluted into two Gaussian peaks, one of the peaks at 1580 cm^{-1} corresponds to the G peak, ascribed to the optical zone center vibration (E_{2g} mode) of all pairs of sp^2 sites in aromatic rings and olefinic chains, and the other is the shoulder peak around 1350 cm^{-1} corresponding to the D peak, which originates from the breathing vibration of sp^2 sites only in rings.[27] Generally, the

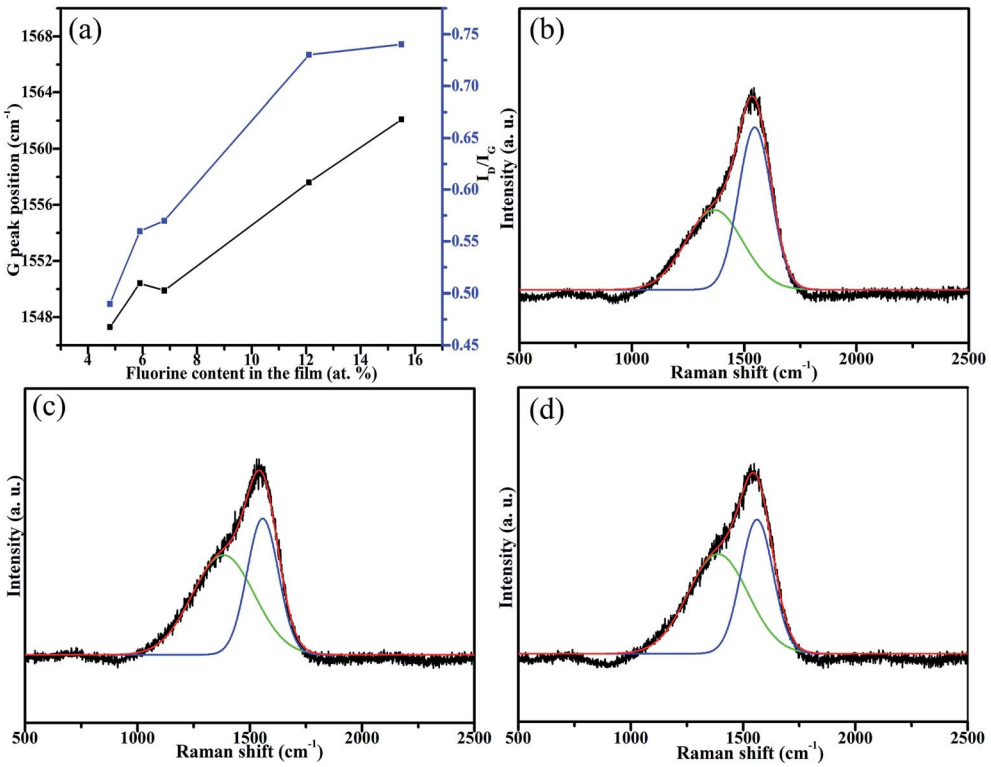

Fig. 3 (a) The plot of G peak position and I_D/I_G obtained from the Raman spectra for the a-C:H:F films with increasing fluorine atomic concentration; (b), (c) and (d) are the Raman spectra for the a-C:H:F films with increasing fluorine contents of 4.8 at%, 12.1 at%, 15.5 at%, correspondingly.

peak intensity ratio (I_D/I_G) falls as the size and number of aromatic rings per cluster decreases and the fraction of chain groups increases. To some extent, the increase of the sp^3/sp^2 ratio comes along with the decrease of I_D/I_G and the size and number of sp^2-clusters.

Fig. 3a shows that the position shift of the G peak spans from 1547 to 1562 cm^{-1} and I_D/I_G changes from 0.49 to 0.74. Raman information is associated with the size and amount of sp^2-hybridized carbon domains. The increase of I_D/I_G indicates the increase in the amount of sp^2 configurations in aromatic rings or olefin C=C bonds, and the slight upward shift of the G peak is ascribed to the increasing sp^2-C phase and the formation of sp^2-hybridized carbon domains. The increase of the intensity ratio of D-band to G-band (I_D/I_G) and the upward shift of the G-band upon increasing the CF_4/CH_4 ratio reveal the increasing amount of sp^2 clusters, confirming the structural changes.[28] The Raman results also indicate that sp^2-hybridized carbon domains are the main component of the C–C network. The addition of fluorine breaks the cross-linked C–C network and collapses the sp^3 diamond-like matrix, thus a new and more open structural arrangement is built.

F-DLC films with a low concentration of fluorine sustain a graphite-like and fullerene-like microstructure. But for high fluorine concentrations, these films have the characteristic of a disordered microstructure arrangement. This can be attributed to the cooperative effect of two aspects. Firstly, the increasing number of C–CF and C–F groups and the emergence of CF_2 groups in large ring and chain patterns terminates the carbon network. Secondly, the proportion of sp^2 phases increases and sp^2 hybridized carbon domains form in the microstructure, which is been supported by the increase in I_D/I_G and the shift of the G peaks to a higher frequency. The breaking of C–C bonding and the formation of sp^2 sites will lead to the formation of disordered rings.

4. Conclusion

The microstructure of films strongly depends on the energies of which the fluorocarbon precursors impact the growing film surface. CH_4 and CF_4 are dissociated and ionized into CH_n and CF_n ($n = 1, 2, 3$) radicals at a fixed voltage of −1000 V, which would impact and react with the surface and subsurface atoms. This process depends on the molecular ion energy. For CH_n^+ ions, this energy is almost totally concentrated in the C atoms, while it is more evenly distributed among all atoms for CF^{3+}. Therefore, hydrocarbon radicals easily impact the surface to promote film deposition. Meanwhile, fluorine coalesces with hydrogen from hydrocarbon radicals to form volatile HF, leaving lots of dangling bonds. These dangling bonds are saturated by carbon-carrying species, finally prompting the growth of fluorocarbon groups. Upon increasing the gas flow ratio of CF_4/CH_4, a larger amount of hydrogen is lost during growth by chemical sputtering, and H from C–H bonds is displaced by incoming fluorine ions. Therefore, as the gas flow

ratio of CF_4/CH_4 increases, the content of fluorine increases, the $-CF_2$ group emerges in the film, the peak width at half height of the C–F bond becomes sharp, and the intensity of the C–F peak increases.

The evolution of microstructure with fluorine content can be explained by the deposition mechanism. According to the subplantation model, on the one hand, the high energy C ion derived from CH_4 has a probability to penetrate the surface, and enter a subsurface interstitial site to form an sp^3 configuration, while a low energy C ion from CF_4 will just stick to the surface, and remain in its lowest energy sp^2 state. On the other hand, the total gas pressure of the reacting gases increases upon increasing the CF_4 gas flow, collisions of carbon-carrying ions will increase and they will lose energy when being accelerated across the sheath, thus increasing the CF_4 gas flow leads to the formation of sp^2 sites on the surface and the growth of films. The Raman results also indicate that sp^2-hybridized carbon domains are the main components of the C–C network. The addition of fluorine breaks the cross-linked C–C network and collapses the sp^3 diamond-like matrix, and thus a new and more open structural arrangement is build.

To conclude, at low fluorine contents, many C sites bond to neighboring C, and the film microstructure displays lots of well organized graphite-like and fullerene-like fragments. As the amount of F incorporated in the network increases, F-terminated large rings, branches and chains with sp^2 sites densify and start to interact with each other, and features like interlocking pores and amorphousness strongly prevail in the microstructure.

Acknowledgements

This work was financially supported by the Major State Basic Research Development Program of China (973 Program) (No. 2013CB632304) and the National Natural Science Foundation of China (Grant no. 51275508, 51205383).

References

1 M. Hakovirta, R. Verda, X. M. He and M. Nastasi, *Diamond Relat. Mater.*, 2001, **10**, 1486–1490.
2 F. R. Marciano, E. C. Almeida, D. A. Lima-Oliveira, E. J. Corat and V. J. Trava-Airoldi, *Diamond Relat. Mater.*, 2010, **19**, 537–540.
3 F. G. Sen, Y. Qi and A. T. Alpas, *Acta Mater.*, 2011, **59**, 2601–2614.
4 J. Robertson, *Tribol. Int.*, 2003, **36**, 405–415.
5 M. Hakovirta, R. Verda, X. M. He and M. Nastasi, *Diamond Relat. Mater.*, 2001, **10**, 1486–1490.
6 T. Hasebe, A. Shimada, T. Suzuki, Y. Matsuoka, T. Saito, S. Yohena, A. Kamijo, N. Shiraga, M. Higuchi, K. Kimura, H. Yoshimura and S. Kuribayashi, *J. Biomed. Mater. Res., Part A*, 2006, **76A**, 86–94.
7 G. Q. Yu, B. K. Tay, Z. Sun and L. K. Pan, *Appl. Surf. Sci.*, 2003, **219**, 228–237.
8 Z. Q. Yao, P. Yang, N. Huang, H. Sun and J. Wang, *Appl. Surf. Sci.*, 2004, **230**, 172–178.
9 L. F. Zhang, F. G. Wang, L. Qiang, K. X. Gao, B. Zhang and J. Y. Zhang, *RSC Adv.*, 2015, **5**, 9635–9649.
10 F. G. Sen, Y. Qi and A. T. Alpas, *J. Mater. Res.*, 2011, **24**, 2461–2470.
11 L. G. Jacobsohn, D. F. Franceschini, M. da Costa and F. L. Freire, *J. Vac. Sci. Technol., A*, 2000, **18**, 2230–2238.
12 F. L. Freire, M. da Costa, L. G. Jacobsohn and D. F. Franceschini, *Diamond Relat. Mater.*, 2001, **10**, 125–131.
13 M. Ishihara, M. Suzuki, T. Watanabe, T. Nakamura, A. Tanaka and Y. Koga, *Diamond Relat. Mater.*, 2005, **14**, 989–993.
14 A. Lamperti and P. M. Ossi, *Appl. Surf. Sci.*, 2003, **205**, 113–120.
15 M. da Costa, F. L. Freire, L. G. Jacobsohn, D. Franceschini, G. Mariotto and I. R. J. Baumvol, *Diamond Relat. Mater.*, 2001, **10**, 910–914.
16 L. G. Jacobsohn, D. F. Franceschini, M. da Costa and F. L. Freire, *J. Vac. Sci. Technol., A*, 2000, **18**, 2230–2238.
17 F. L. Freire Jr, M. E. H. Maia da Costa, L. G. Jacobsohn and D. F. Franceschini, *Diamond Relat. Mater.*, 2001, **10**, 125–131.
18 A. Bendavid, P. J. Martin, L. Randeniya and M. S. Amin, *Diamond Relat. Mater.*, 2009, **18**, 66–71.
19 T. Hasebe, S. Nagashima, A. Kamijo, T. Yoshimura, T. Ishimaru, Y. Yoshimoto, S. Yohena, H. Kodama, A. Hotta, K. Takahashi and T. Suzuki, *Thin Solid Films*, 2007, **516**, 299–303.
20 J. Robertson, *Mater. Sci. Eng., R*, 2002, **37**, 129–281.
21 A. Lamperti and P. M. Ossi, *Appl. Surf. Sci.*, 2003, **205**, 113–120.
22 A. Lamperti, C. E. Bottani and P. M. Ossi, *J. Am. Soc. Mass Spectrom.*, 2005, **16**, 126–131.
23 Q. Wang, C. Wang, Z. Wang, J. Zhang and D. He, *Appl. Phys. Lett.*, 2007, **91**, 141902–141903.
24 C. Goyenola, S. Stafstrom, S. Schmidt, L. Hultman and G. K. Gueorguiev, *J. Phys. Chem. C*, 2014, **118**, 6514–6521.
25 C. Ronning, M. Buttner, U. Vetter, H. Feldermann, O. Wondratschek, H. Hofsass, W. Brunner, F. C. K. Au, Q. Li and S. T. Lee, *J. Appl. Phys.*, 2001, **90**, 4237–4245.
26 A. C. Ferrari and J. Robertson, *Phys. Rev. B: Condens. Matter Mater. Phys.*, 2000, **61**, 14095–14107.
27 A. C. Ferrari and J. Robertson, *Phys. Rev. B: Condens. Matter Mater. Phys.*, 2001, **64**, 075414.
28 G. Irmer and A. Dorner-Reisel, *Adv. Eng. Mater.*, 2005, **7**, 694–705.

